U.P.B. Sci. Bull., Series A, Vol. 82, Iss. 3, 2020 ISSN 1223-7027

PROPORTIONAL AND BANG-BANG CONTROLLER FOR SPACE VEHICLE DE-TUMBLING USING QUATERNION-BASED ATTITUDE DETERMINATION

Florin MINGIREANU[1], Laurentiu BASCHIR[2], Sorin MICLOS[3], Dan SAVASTRU[4], Nicolae JULA[5]

Attitude determination and control of a space vehicle is an important task that can make the difference between a failed and successful mission. Many types of sensors and actuators are employed in order to achieve good performance in attitude determination and control. Upon deployment from the launcher a space vehicle needs to determine its attitude and then control it in an agile way. Technologically it is impossible to separate the space vehicle without any residual angular velocities. Hence, a de-tumbling procedure needs to be performed to prepare the space vehicle for its subsequent mission. An agile de-tumbling is needed to save fuel and energy resources onboard the space vehicle. Our research team has developed an in-house software package written in FORTRAN that allows accurate simulation of attitude determination and control for space vehicles. The attitude is represented in the body reference system and the attitude solution is evolved using a quaternion-based formulation. Torques is included as user defined parameters. For the current work the focus is kept on control torques which is assumed to be significantly larger than the external perturbatory torques, a condition needed for an agile attitude control system.

Keywords: tumbling, attitude determination, space vehicle.

1. Introduction

Human and non-human space vehicles have been used since the beginning of space age [1,2]. A space vehicle can fulfill a wide range of missions such as: Earth surveillance [3], satellite inspection [4], experimental payload deployment, deep space exploration missions (e.g. Moon, Mars) [5].

Typically a space vehicle is injected onto the desired trajectory using a launcher system. A European launcher system typically used for small and medium payloads is the 4 stage Vega vehicle – Fig. 1.

[1] PhD, Romanian Space Agency, Romania, e-mail: florin.mingireanu@rosa.ro
[2] PhD Eng., National Institute of R&D for Optoelectronics INOE 2000, Romania, e-mail: baschirlaurentiu@inoe.ro
[3] PhD Eng., National Institute of R&D for Optoelectronics INOE 2000, Romania, e-mail: miclos@inoe.ro
[4] PhD Eng., National Institute of R&D for Optoelectronics INOE 2000, Romania, e-mail: dsavas@inoe.ro
[5] Prof., Military Technical Academy, Romania, e-mail: nicolae.jula@gmail.com

Fig. 1 Vega space launcher [6].

Regardless of the type of launcher, upon injection on its desired trajectory a space vehicle can have some residual angular velocities around 1, 2 or all 3 axes. In order to accurately fulfill its mission the space vehicle needs to decrease the angular velocities to zero or to some controlled values acceptable for the mission for which it is intended. The operation of eliminating the residual angular velocities is named de-tumbling [6] and represents an important phase in the overall mission since the success of the mission depends upon the successful de-tumbling procedure.

2. Quaternion formulation for attitude solution

The body reference system associated with a space vehicle is shown in Fig. 2 [7-11].

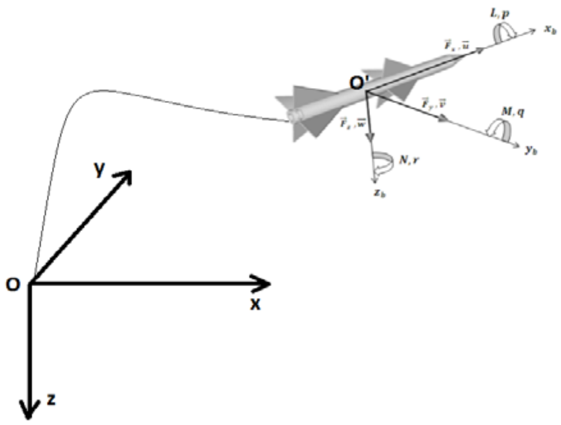

Fig. 2. The system of reference.

A set of 3 coupled differential equations can be written in order to describe the attitude dynamics of the space vehicle. The 3 coupled differential equations represent only half of a full 6 DOF model [12].
The attitude dynamics equations written in vector form are as it follows [12-15]:

$$\frac{d\vec{K}}{dt} \equiv \frac{\partial \vec{K}}{\partial t} + \vec{\Omega} \times \vec{K} = \sum_i \vec{H}_i + \vec{H}_T \tag{1}$$

The matrix form of vector equations (1) can be written as it follows:

$$\begin{bmatrix} p \\ q \\ r \end{bmatrix} = I^{-1} \left\{ H_0 \begin{bmatrix} C_l^A \\ C_m^A \\ C_n^A \end{bmatrix} + H_{T0} \begin{bmatrix} C_l^T \\ C_m^T \\ C_n^T \end{bmatrix} \right\} - I^{-1} \begin{bmatrix} (B-C)qr \\ (C-A)rp \\ (A-B)pq \end{bmatrix} \tag{2}$$

For a space vehicle we assume that aerodynamic torques is negligible and hence equations (2) become:

$$\begin{bmatrix} p \\ q \\ r \end{bmatrix} = I^{-1} \left\{ H_{T0} \begin{bmatrix} C_l^T \\ C_m^T \\ C_n^T \end{bmatrix} \right\} - I^{-1} \begin{bmatrix} (B-C)qr \\ (C-A)rp \\ (A-B)pq \end{bmatrix} \tag{3}$$

This assumption can still be true even in the presence of aerodynamic torques if the control torques is significantly larger than the aerodynamic torques.

Instead of using Euler formulation for the rotation between the body reference frame and the inertial reference frame, we choose the quaternion base formulation. The advantage of the quaternion based formulation is that it does not exhibit any trigonometric singularities providing lock free formulation when compared to Euler formulation [12].

The direct matrix of rotation A_i is [9, 10]:

$$A_i = \begin{bmatrix} q_4^2 + q_1^2 - q_2^2 - q_3^2 & -2(q_1q_2 + q_3q_4) & -2(q_3q_1 - q_2q_4) \\ 2(q_1q_2 - q_3q_4) & -q_4^2 - q_2^2 + q_3^2 + q_1^2 & -2(q_2q_3 + q_4q_1) \\ 2(q_1q_3 + q_2q_4) & -2(q_2q_3 - q_4q_1) & -q_4^2 - q_3^2 + q_1^2 + q_2^2 \end{bmatrix} \tag{4}$$

while the inverse matrix of rotation B_i is the transpose of A_i i:

$$B_i = \begin{bmatrix} q_4^2 + q_1^2 - q_2^2 - q_3^2 & 2(q_1q_2 - q_3q_4) & 2(q_3q_1 + q_2q_4) \\ -2(q_1q_2 + q_3q_4) & -q_4^2 - q_2^2 + q_3^2 + q_1^2 & -2(q_2q_3 - q_4q_1) \\ -2(q_1q_3 - q_2q_4) & -2(q_2q_3 + q_4q_1) & -q_4^2 - q_3^2 + q_1^2 + q_2^2 \end{bmatrix} \tag{5}$$

The relations between Euler angles and quaternions are given as it follows [12]:

$$\begin{aligned} q_1 &= -\cos\frac{\varphi}{2}\cdot\sin\frac{\theta}{2}\cdot\sin\frac{\psi}{2}+\sin\frac{\varphi}{2}\cdot\cos\frac{\theta}{2}\cdot\cos\frac{\psi}{2} \\ q_2 &= \cos\frac{\varphi}{2}\cdot\sin\frac{\theta}{2}\cdot\cos\frac{\psi}{2}+\sin\frac{\varphi}{2}\cdot\cos\frac{\theta}{2}\cdot\sin\frac{\psi}{2} \\ q_3 &= \cos\frac{\varphi}{2}\cdot\cos\frac{\theta}{2}\cdot\sin\frac{\psi}{2}-\sin\frac{\varphi}{2}\cdot\sin\frac{\theta}{2}\cdot\cos\frac{\psi}{2} \\ q_4 &= \cos\frac{\varphi}{2}\cdot\cos\frac{\theta}{2}\cdot\cos\frac{\psi}{2}+\sin\frac{\varphi}{2}\cdot\sin\frac{\theta}{2}\cdot\sin\frac{\psi}{2} \end{aligned} \tag{6}$$

In an attitude control system a 3D gyroscope is typically used. The signals of the gyroscope for each of its axis represent the angular velocities in the body reference system.

The equations that connect the gyroscope signals to the time derivative of quaternions are [12, 14, 16]:

$$\begin{bmatrix} p & q & r \end{bmatrix}^T = U_q \begin{bmatrix} \dot{q}_1 & \dot{q}_2 & \dot{q}_3 \end{bmatrix}^T \tag{7}$$

where

$$U_q = 2\begin{bmatrix} q_4+\frac{q_1^2}{q_4} & q_3+\frac{q_2 q_1}{q_4} & -q_2+\frac{q_3 q_1}{q_4} \\ -q_3+\frac{q_1 q_2}{q_4} & q_4+\frac{q_2^2}{q_4} & q_1+\frac{q_3 q_2}{q_4} \\ q_2+\frac{q_1 q_3}{q_4} & -q_1+\frac{q_2 q_3}{q_4} & q_4+\frac{q_3^2}{q_4} \end{bmatrix} \tag{8}$$

Hence, the full attitude kinematics in quaternion formulation is as follows:

$$\begin{bmatrix} \dot{q}_1 \\ \dot{q}_2 \\ \dot{q}_3 \\ \dot{q}_4 \end{bmatrix} = \frac{1}{2}\begin{bmatrix} 0 & r & -q & p \\ -r & 0 & p & q \\ q & -p & 0 & r \\ -p & -q & -r & 0 \end{bmatrix}\begin{bmatrix} q_1 \\ q_2 \\ q_3 \\ q_4 \end{bmatrix} = \frac{1}{2}\begin{bmatrix} q_4 & -q_3 & q_2 \\ q_3 & q_4 & -q_1 \\ -q_2 & q_1 & q_4 \\ -q_1 & -q_2 & -q_3 \end{bmatrix}\begin{bmatrix} p \\ q \\ r \end{bmatrix} \tag{9}$$

A free tumbling space vehicle dynamics would be characterized by the differential equations (3) in which we set all control torques to zero values:

$$H_{T0}\begin{bmatrix} C_l^T \\ C_m^T \\ C_n^T \end{bmatrix} = \begin{bmatrix} \tau_1 \\ \tau_2 \\ \tau_3 \end{bmatrix} = 0 \tag{10}$$

This is the case of the space vehicle dynamics just after the separation from the launcher.

In order to de-tumble the space vehicle a coordinated set of correction torques τ_1, τ_2, τ_3 have to be applied as functions of time such that the angular velocities of the space vehicle are reduced to zero.

A solution is to apply proportional correction torques such as:

$$\begin{bmatrix} \tau_1 \\ \tau_2 \\ \tau_3 \end{bmatrix} = \begin{bmatrix} -k_1 p \\ -k_2 q \\ -k_3 r \end{bmatrix} \tag{11}$$

where k_1, k_2, k_3 are proportional control coefficients. Another technologically simpler solution is to use a bang-bang type of controller where the torques τ_1, τ_2, τ_3 have non-zero values if the corresponding angular velocity is larger than a threshold value. The bang-bang controller is simpler to be implemented than the proportional correction torques controller. However, for longer missions the proportional correction torques controller might exhibit lower fuel/energy consumption.

3. Numerical model and initial conditions

A FORTRAN code was developed using the differential equations for quaternion-based attitude solution (2), (4), (5), (8) and (9) [17-23]. The code block structure is shown in Fig. 3.

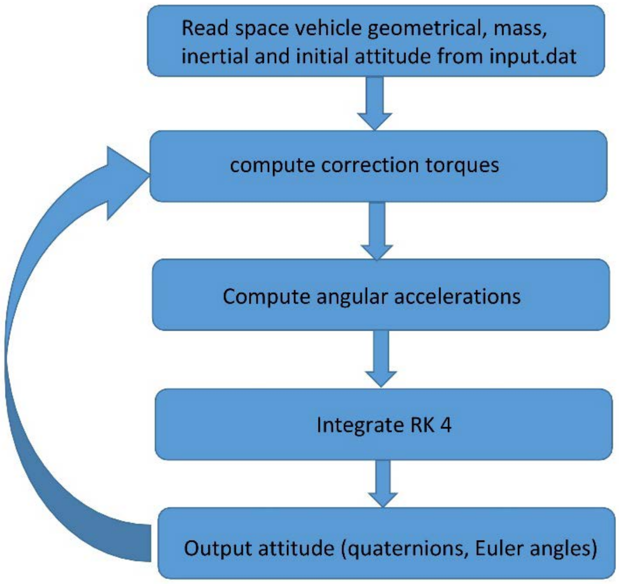

Fig. 3. Attitude block control.

The FORTRAN code uses an input file named INPUT.dat that contains the main characteristics of the space vehicle: initial angular velocities, initial attitude angles, moments of inertia.

Upon running the FORTRAN code the results are stored in several output files which store pitch, yaw, roll angles and pitch control torque, roll control torque and yaw control torque. The user can view these values using GNUPLOT.

The numerical examples were run using a slender body space vehicle with INPUT.dat characteristics shown in Table 1.

For each case (Case 1, Case 2 and Case 3) shown in Table 1 there were 2 simulations performed. One simulation used the proportional controller as described by equation (11) while the second simulation used the bang-bang controller with a dead-band for all angular velocities of 0.01 degrees/second. Roll, yaw and pitch angles as functions of time are displayed for each simulation. At the same time, the control torques as functions of times are also displayed for each simulation in order to assess the effectiveness of each control technique for each of the cases.

Table 1

Space vehicle characteristics INPUT.dat

Name	Case 1	Case 2	Case 3
Roll angle (°)	0.0	20.0	20.0
Pitch angle (°)	0.0	0.0	15.0
Yaw angle (°)	0.0	0.0	23.0
Roll rate (°/s)	100.05	100.05	100.05
Pitch rate (°/s)	0.0	119.9	119.9
Yaw rate (°/s)	0.0	0.0	90.0
Roll moment of inertia (kg/m^2)	0.1499	0.1499	0.1499
Pitch moment of inertia (kg/m^2)	41.58	41.58	41.58
Yaw moment of inertia (kg/m^2)	41.58	41.58	41.58

4. Numerical results

Proportional and Bang-bang controller are distinctly considered.

Proportional controller

For all cases (Case 1, Case 2 and Case 3) a proportional controller was used with the proportional coefficients given by the following equation:

$$k_1 = k_2 = k_3 = -1.7 \tag{12}$$

The proportional coefficients were chosen to be equal in order to simplify a potential technological implementation of the de-tumbling controller. The total simulation time was 333 seconds which was found to be more than enough for the de-tumbling procedure.

For the **Case 1**, in Fig. 4, Fig 5 and Fig. 6 it can be noticed that the roll, pitch and yaw angles become constant after a time of about 50 seconds. At the same time the roll, pitch and yaw angle rates become zero. That moment corresponds to the de-tumbling moment of the studied space vehicle.

It can also be noticed that the de-tumbling occurs only on the roll axis since the initial angular velocity for Case 1 has only a roll component.

There a no correction torque acting on pitch and yaw axis since there is no angular velocity component on those axis. The roll angle is stabilized at about 150 degrees after 50 seconds. After 50 seconds the de-tumbling procedure ends.

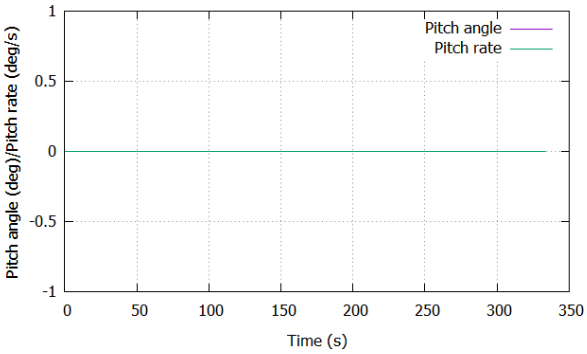

Fig. 4 Case 1 - Pitch angle and pitch rate.

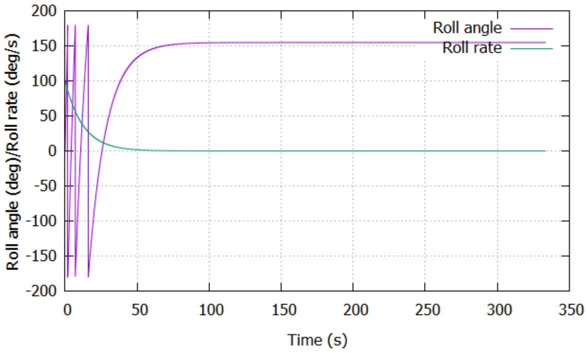

Fig. 5 Case 1 - Roll angle and roll rate.

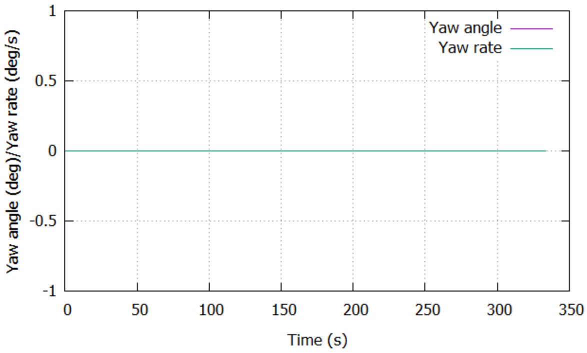

Fig. 6 Case 1 - Yaw angle and yaw rate.

For the **Case 2**, in Fig. 7, Fig 8 and Fig. 9 it can be noticed the roll, pitch and yaw angles and their respective rates. In this case it was considered that the space vehicle has some residual angular velocities on both roll and pitch axis and no residual angular velocity on yaw axis. At the same time, the space vehicle is considered to start from a roll angle of 20 degrees in the positive direction.

Although the space vehicle initially has residual angular velocities only on the pitch and roll axis, due to the coupling dynamics we can notice the yaw axis angular velocity also becomes non-zero. However, the de-tumbling procedure is able to cope with this and after about 150 seconds the roll, pitch and yaw angular rates are stabilized to zero degrees per second. Hence, the de-tumbling procedure successfully de-tumbles the space vehicle in about 150 seconds.

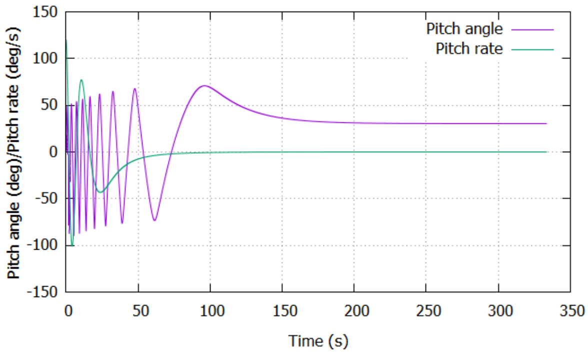

Fig. 7 Case 2 - Pitch angle and pitch rate.

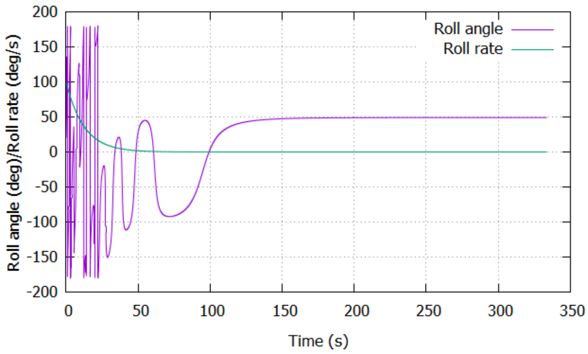

Fig. 8 Case 2 - Roll angle and roll rate.

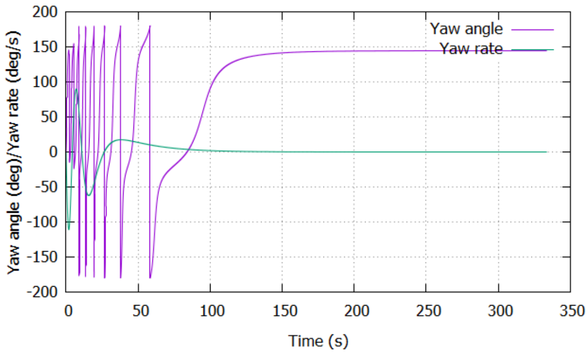

Fig. 9 Case 2 - Yaw angle and yaw rate.

For the **Case 3**, in Fig. 10, Fig 11 and Fig. 12 it can be noticed the roll, pitch and yaw angles and their respective rates. In this case the space vehicle is assumed to have non-zero initial angular velocities on all axes (roll, pitch and yaw). At the same time, the space vehicle is also assumed to have non-zero initial angles on roll, pitch and yaw axis.

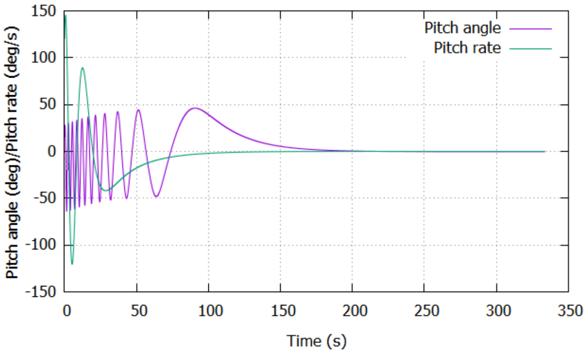

Fig. 10 Case 3 - Pitch angle and pitch rate.

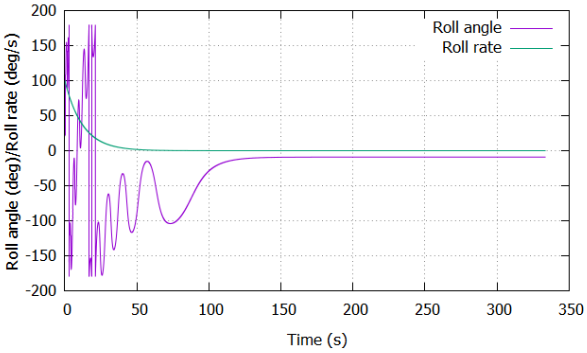

Fig. 11 Case 3 - Roll angle and roll rate.

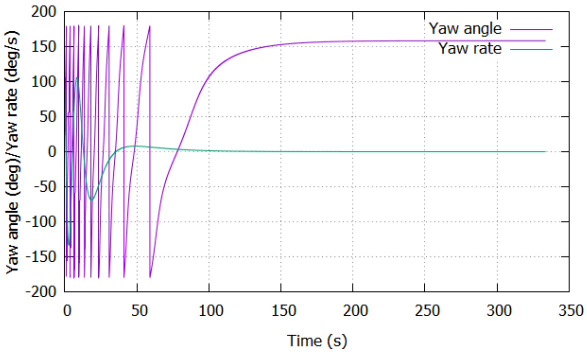

Fig.12 Case 3 - Yaw angle and yaw rate.

From Fig. 10, 11 and 12 it can be noticed that the de-tumbling in Case 3 occurs after about 150 seconds when the angular rates around all axes become 0

°/s. Since in Case 3 the space vehicle has non-zero initial angles and non-zero initial angular rates it can be concluded that the de-tumbling procedure is able to de-tumble the space vehicle despite the complex coupled dynamics.

Bang-bang controller

From the numerical simulations shown for the proportional controller it can be seen that the proportional controller is able to de-tumble a space vehicle even when all axes exhibit initial angular velocities due to the separation of the space vehicle from the launcher. A bang-bang controller has the advantage of being simpler to implement than a proportional controller. Hence, its performance needs to be analyzed compared to the performance of a more complex proportional controller which was already shown to exhibit excellent de-tumbling capabilities.

In order to assess the performance of a bang-bang controller, Case 3 was chosen as a baseline being the most complicated case from the 3 cases presented. The bang-bang controller was implemented with equal correction torques $\tau_1 = \tau_2 = \tau_3$ on all 3 axes (roll, pitch, yaw). The dead-band in angular velocity on each axis was set to 1 °/s. Fig. 13, 14 and 15 shows the pitch, roll and yaw angles and their respective time derivatives (pitch, roll, and yaw rates).

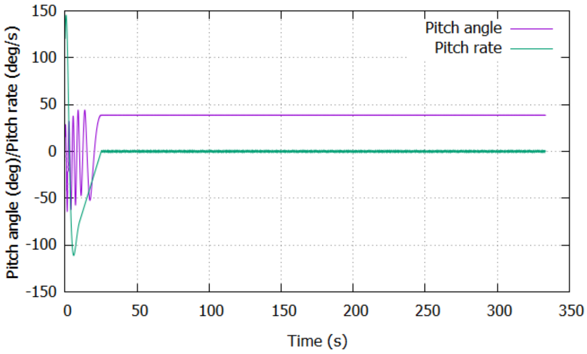

Fig. 13 Bang-bang controller - Pitch angle and pitch rate.

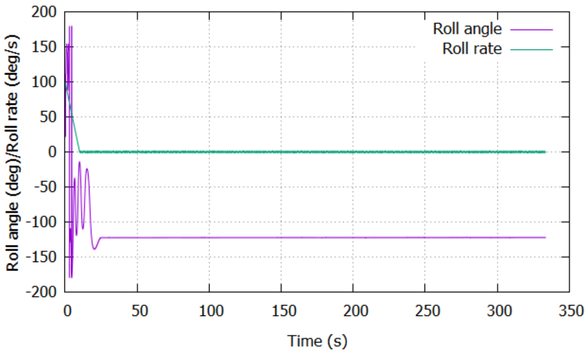

Fig. 14 Bang-bang controller – Roll angle and roll rate.

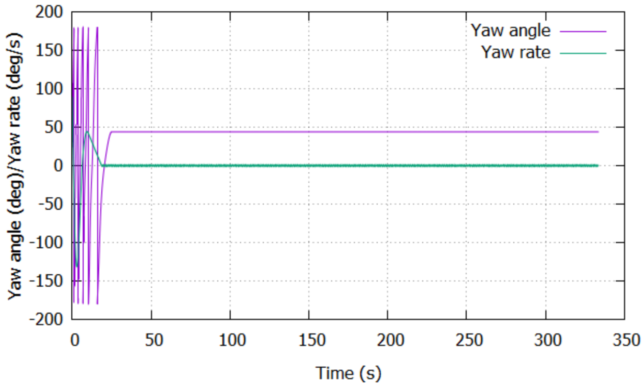

Fig. 15 Bang-bang controller – Yaw angle and yaw rate.

The bang-bang controller de-tumbles faster the space vehicle. However, after de-tumbling the vehicle will be rocking back and forth on each axis with an angular velocity smaller than the dead-band. The torque activation after de-tumbling can be observed in Fig. 16 where after 50 s, when the space vehicle is de-tumbled according to Fig. 13, 14, 15, the torque is still used in order to maintain the space vehicle within the allowed dead-band for the angular velocities. Fig. 16 shows the roll torque for the bang-bang controller while Fig. 17 shows the roll torque for the proportional controller.

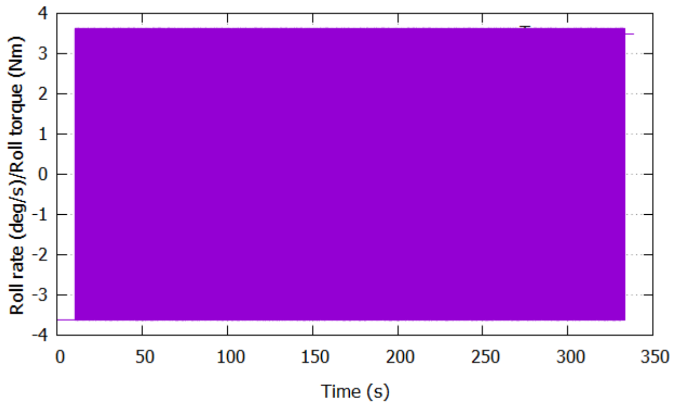

Fig. 16 Torque activation for bang-bang controller.

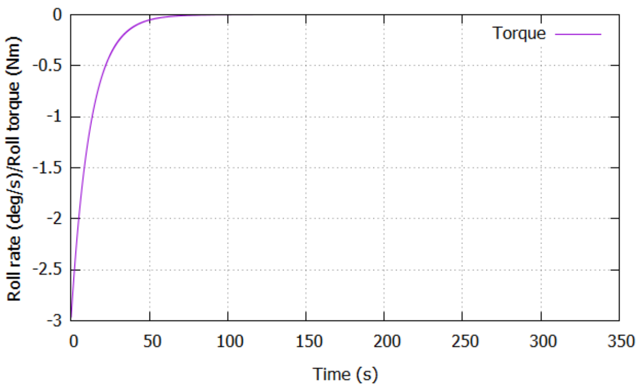

Fig. 17 Torque activation for proportional controller.

From Fig. 16 and 17 it can be noticed that the fuel consumption of a bang-bang controller is higher than the fuel consumption of a proportional controller.

The advantage of the bang-bang controller is that it offers a technological simplification. In a bang-bang controller simpler actuators can also be used since they only need to be ON or OFF.

5. Conclusions

A FORTRAN code is developed based on attitude dynamics and kinematics equations with quaternion based formulation.

The FORTRAN code allows the comparison between various types of controllers for the de-tumbling procedure of a space vehicle.

The in-house developed software allows great flexibility in analyzing typical de-tumbling procedures for various space vehicles without the limitation of commercial packages.

Proportional controller is compared with a bang-bang controller and while the bang-bang controller is simpler than the proportional controller we conclude that the proportional controller exhibits lower fuel/energy consumption which is relevant for a longer mission.

The current work presents the basis of a future potential de-tumble controller for space vehicle missions, including translunar and trans-Mars missions.

Acknowledgments

The authors are also grateful for the support of European Space Agency (ESA) and Romanian Space Agency (ROSA), 98 MANUNET/2019 and Project No. PN 18N/2020 throughout the activities of this project.

REFERENCES

[1] *Burrows, W. E.*, This New Ocean : The Story of the First Space Age, Random House, 1 ed., 1998, ISBN-13: 978-0679445210.

[2] Sounding Rockets Program Office, „NASA Sounding Rockets User Handbook", NASA Goddard Space Flight Center, July 2015.

[3] https://en.wikipedia.org/wiki/Earth_observation_satellite

[4] https://en.wikipedia.org/wiki/Project_SAINT

[5] *Goodliff, K., Cirillo, W., Mattfeld, B., Stromgren, C., and Shyface, H.*, "Comparison of Human Exploration Architecture and Campaign Approaches", NASA Technical Report Server, https://ntrs.nasa.gov/archive/nasa/casi.ntrs.nasa.Gov/ 20160006315.pdf

[6] https://www.arianespace.com/vehicle/vega/

[7] *Hughes, P. C.*, Spacecraft attitude dynamics, John Wiley & Sons, Inc., New York, 1986.

[8] *Servidia, P. A., Sanchez-Pena, R. S.*, "Thruster design for position/attitude control of spacecraft", IEEE Transactions on Aerospace Engineering, **vol. 38**, No. 4, ISSN: 0018-9251, 2002.

[9] *Pontani, M., Cappelletti, C.*, "CubeSat Collision Risk Analysis at Orbital Injection", AAS/AIAA Astrodynamics Specialist Conference, Kauai, USA, Volume: Advances in the Astronautical Sciences, **vol. 148**, pp. 3111-3130, 2013.

[10] *Radix,J.C.*, Systemes inertiels a composants lies "Strap Down", Cepadues-Editions, Ecole Nationale Superieure de lAeronautiques et de l,Espace SUPAERO, Toulouse, 1993.

[11] *Cybulski, R. J., Shellhammer, D. M., Lovell, R. R., Domino, E. J., Kotnik, J. T.*, "Results from SERT I ion rocket flight test", NASA Technical report server, 1965.

[12] *Zipfel, P. H.*, "Modeling and simulation of aerospace vehicle dynamics", 3rd Edition, ISBN: 978-1-62410-250-9, American Institute of Aeronautics and Astronautics, 2014.

[13] *Salychev,O.S.*, „Inertial Systems in Navigation and Geophysics", Bauman MSTU Press, Moscow, 1998.

[14] *Starin, S. R.*, "Attitude determination and control systems", NASA Goddard Space Flight Center, 2011.

[15] *Schmidt, M. and Schilling, K.* „Formation flying techniques for pico-satellites", 6th International Workshop on Satellite Constellation and Formation Flying, 2010

[16] *Zimpfer, D., Hattis, P., Gavert, D.*, "Space shuttle GN&C development history and evolution", NASA Technical report https://ntrs.nasa.gov/archive/nasa/casi.ntrs.nasa.gov/20110014833.pdf (accessed March, 24 2020)

[17] *Mingireanu, F., and Jula, N.*, "High altitude UAV development and flight testing", International Astronautical Congress, Adelaide, Australia, 2017, IAC-17.D2.6.4.

[18] *Mingireanu, F, and Jula, N.,* “Numerical modelling of trajectory of high altitude missions,” Journal of Aerospace Science and Technology, David Publishing Company, 2015. doi:10.17265/2332-8258/2015.02.002

[19] *S. Miclos, D. Savastru, R. Savastru, I. I. Lancranjan,* Numerical analysis of long period grating fibre sensor fabrication using thermal processing, J. Optoelectron. Adv. M., Vol. 20, no. 1-2, January –February, pp. 20-26, 2018

[20] *D. XUE, R. PAN, L. WANG, H. DENG, Y. LYU, Q. XUE, J. HAN,* A numerical approach for designing multi-wavelength plate, J. Optoelectron. Adv. M., Vol. 20, no. 5 - 6, May – June pp. 253 – 257, 2018

[21] *Zoran M., Savastru D., Miclos S., Tautan M. N., Baschir L.,* Multisensor satellite remote sensing data for heat waves assessment in metropolitan region, J. Optoelectron. Adv. M., Vol. 13, no. 9-10, pp. 1159-1166, Sept-Oct, 2011

[22] *Popescu Aurelian A., Baschir Laurentiu, Savastru Dan, Stafe Mihai, Vasile Georgiana C., Miclos, Sorin, Negutu Constantin, Mihailescu Mona, Puscas Niculae N.,* Analytical considerations and numerical simulations for surface plasmon resonance in four layers plasmonic structures which contain high refractive index waveguide, U.P.B. Sci. Bull., Series A, Vol. 77, Iss. 4, pp. 233-244, 2015

[23] *Mingireanu, F., Jula N., Miclos S., Savastru D. and Baschir L.,* “Solid rocket motors internal ballistic model with erosive and condensed phase considerations”, U.P.B. Sci. Bull., Series A, **Vol. 80**, Iss. 4, 2018